Capacitive mixing for the extraction of energy from salinity differences: Survey of experimental results and electrochemical models

D. Brogioli *, R. Ziano, R.A. Rica, D. Salerno, F. Mantegazza

Dipartimento di Scienze della Salute, Università degli Studi di Milano-Bicocca, Via Cadore 48, Monza (MB) 20900, Italy

ABSTRACT

The "capacitive mixing" (CAPMIX) technique is an emerging technology aimed at the extraction of energy from salinity differences, e.g. between sea and river waters. CAPMIX benefits from the voltage rise that takes place between two electrodes dipped in a saline solution when its salt concentration is changed. Several kinds of electrodes have been proposed so far: activated carbon materials (Brogioli, 2009), membrane-based ion-selective electrodes (Sales et al., 2010), and battery electrodes (Biesheuvel and van der Wal, 2010). The power production mainly depends on two properties of each single electrode: the amplitude of the potential rise upon salinity change, and the potential in the high-salinity solution. The various electrode materials that have been used returned different values of the two parameters, and hence to different power productions. In this paper, we apply electrokinetic and electrochemical models to qualitatively explain the experimentally observed behaviors of various materials under different experimental conditions. The analysis allows to devise techniques for tailoring new materials, particularly suited for the CAPMIX technique.

1. Introduction

Naturally occurring salinity differences can be used for generating completely clean and renewable energy [1–3]. For example, each liter of river water dispersed into the sea corresponds to a free energy loss of around 2.3 kJ, and a significant fraction of this energy can be intercepted and converted into electrical energy. Considering all the rivers, the global potential of this source of energy is around 1 TW [4], a relevant fraction of the whole energy demand. Brines can also be locally available: for example, salt lakes (e.g. Dead Sea) [5], coal-mine brines [6] produced by dissolving geological deposits, or salterns [7]. They can be used *versus* sea water, thus avoiding the fresh water consumption.

Salinity differences can also be produced by distillation. The required heat can be obtained by a renewable source (e.g. by means of a solar concentrator) [8], or can be the waste heat from an industrial process, or part of a co-generation process. Also in this case, the technique contributes to the production of renewable and clean energy.

The key point of the above described processes is the conversion of the salinity difference into electrical current. Known techniques include pressure-retarded osmosis (PRO) [9–11] and reverse electrodialysis (RED) [12,13]. In PRO, a semi-permeable membrane is interposed between the salt and fresh water, generating an osmotic water flow that is fed to a turbine. In RED, the membranes are permeable to either positive or negative ions; the ion diffusion across them constitutes a current that can be extracted.

A new technique, called "capacitive mixing" (CAPMIX) has been recently introduced [14–19]. This technique performs the mixing process of the two solutions in a controlled way, generating an electrical current by periodically switching between the high-salinity and the low-salinity feed solutions the liquid in which a couple of activated carbon electrodes is dipped. The two electrodes immersed in a ionic solution form a so-called supercapacitor. When it is charged by means of an external device, the electrical charge is stored in the electric double layers (EDLs) that develop on the interface between the carbon and the solution. The EDLs are formed by the charges on the surface of the carbon and the distribution of ions that screens the surface charge. The observation that lead to the CAPMIX technique is the fact that the potential difference across the EDLs increases when the solution salinity is decreased at constant charge. This happens because the counter-ions (ions with charge opposite to that in the surface) in the diffuse part of the EDL move away from the electrode, against the electric field, thus increasing the accumulated electrostatic energy at the expense of the free energy of the solutions: this phenomenon has been called "capacitive double layer expansion" (CDLE).

This energy surplus can be extracted by means of the CAPMIX cycle, sketched in Fig. 1a. In CDLE, the cycle begins with the cell filled with the high-salinity solution. The steps are four:

A The cell is charged by means of an external device.
B The circuit is opened. The solution in the cell is substituted with the low-salinity feed solution.
C The cell is discharged through a load; the electrical current flows in the opposite direction with respect to step A.
D The circuit is opened. The liquid in the cell is substituted with the high-salinity feed solution.

Fig. 1b shows the voltage *versus* charge graph for this cycle. During step A, the cell voltage increases, and an electrical charge is temporarily stored in the EDLs. The solution change that takes place in step B, in open circuit, induces a cell voltage rise ΔV. The stored charge is recovered in step C, at a higher voltage with respect to step A. For this reason, due to the voltage rise, the curve encloses an area, which represents the extracted energy.

During step A, the ions coming from the solution at higher salinity are temporarily stored into the electrodes, and they are
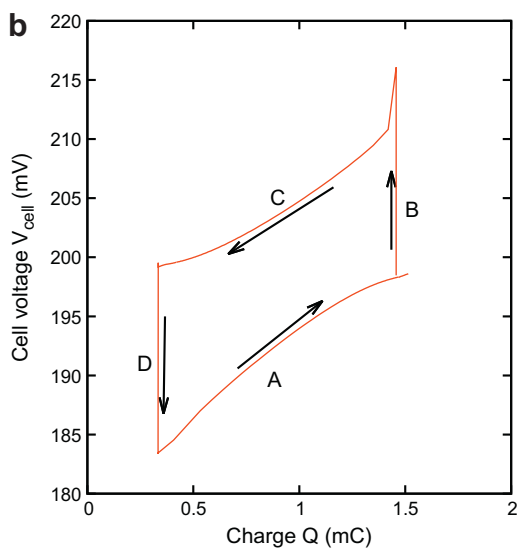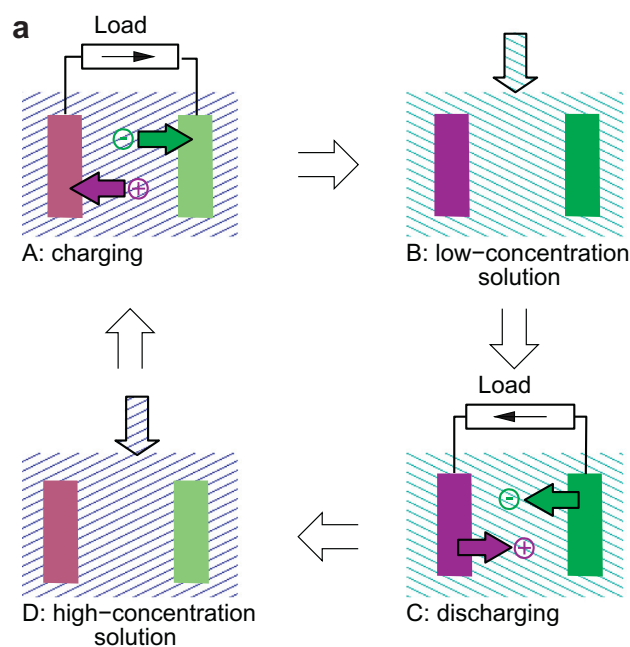

later released into the solution at lower salinity during step C, thus decreasing the total salinity difference. This process can be described as a capacitor-mediated mixing, hence the name "capacitive mixing". It is worth noting that the decrease of the salinity difference between the solutions would take place also if any mechanical unwanted mixing is completely avoided in steps B and D. It is thus evident that the energy is extracted at the expense of the free energy of the solutions; indeed, it has been shown that the voltage rise is connected with the ability of the electrodes to store the salt inside them, when they are charged during phase A [20].

The unwanted mixing taking place when the solution is changed, in steps B and D, reduces the energy efficiency, i.e. the ratio between the extracted energy and the available free energy of the solutions. The Carnot-like cycle described in Ref. [21], which completely avoids any non-capacitive mixing, would be able, at least theoretically, to extract all the free energy of the feed solutions: for example, an energy up to 1.3 kJ can be obtained by using 1 l of 20 mM and 1 l of 500 mM solutions of NaCl. The energy of 2.3 kJ, corresponding to the mixing of 1 l of pure water in an infinite quantity of 500 mM NaCl solution, can be approached by using a finite but large amount of salt water, e.g. with 10 l of 500 mM solution the theoretically produced energy, with the Carnot-like cycle, is 2.2 kJ.

In the initial experiments on CAPMIX a power output up to 10 mW per square meter of electrode was obtained. The main limitation was the charge leakage.

We recently showed that it is possible to avoid the leakage by exploiting non-ideal behaviors of various activated carbon materials (i.e., those behaviors deviating from the ideal polarization) and using suitable couples of different activated carbon materials for the two electrodes [22]. Moreover, the initial results on CAPMIX stimulated other groups to work on similar techniques, based on the very same cycle but with different electrodes. The electrodes that have been proposed are membrane-based ion-selective electrodes [15] (not studied in the present paper) and battery electrodes [23]. In all the cases, the cell is actually an accumulator (i.e. a capacitor or a battery): it is thus evident that such techniques belong to the same family of CAPMIX, although the technique based on battery electrodes could be better referred to as an "accumulator mixing" techniques. The new materials allowed to reach a power production up to 200 mW per square meter of electrode. See Refs. [18,19] for reviews of the CAPMIX techniques. It is worth noting that CAPMIX can be interpreted as the reverse of a desalination process, in particular, capacitive deionization [24], membrane capacitive deionization [25] and desalination batteries [26].

Many efforts have been done in order to improve the power production of CAPMIX technique; in particular, available studies focus on alternative schemes of electrical charging and discharging [27], alternative electrode geometries [28,29] and modeling of the electrokinetics inside the electrodes [30–33].

The target of the present paper is to discuss the models that qualitatively describe the experimental results. One of the most relevant parameters of the CAPMIX cell is the voltage rise, i.e., the voltage increase that takes place during the switching of the solutions in the cell. This parameter is defined in Section 2. The experimental results for the CDLE technique obtained with carbon and battery electrodes are sumarized in Section 3. Finally, the models that describe all these observations are presented and discussed in Section 4.

2. Electrode potential rise and cell voltage rise

The graph in Fig. 2 shows the potentials $\varphi_+(t)$ and $\varphi_-(t)$ of the two electrodes ($\varphi_+(t) > \varphi_-(t)$) as a function of time during a CAP-

Fig. 1. The CAPMIX cycle. Panel a: sketch of the cycle. Panel b: representation of the cycle in the voltage *versus* charge graph. The phases are: A, charging; B, flow of low-salinity solution; C, discharging; and D, flow of high-salinity solution.

MIX cycle, together with the cell voltage $V_{cell}(t) = \varphi_+(t) - \varphi_-(t)$. In the work presented in this paper, all the potentials were measured with respect to an Ag/AgCl reference electrode with 3 M concentration of AgCl.

During step A (charging), the electrodes are connected to a power supply generating the external voltage V_{ext}, through a load resistor R_{load}, while dipped in the high-salinity feed solution. During this step, the cell voltage asymptotically approaches the external voltage, i.e. $V_{cell} \approx V_{ext}$, and the electrodes reach the potentials φ_+^H and φ_-^H. In the following, the potential in the high-salinity solution, i.e. $\varphi_\pm^H$, will be called "base potential".

During step B, the circuit is opened and the solution in the cell is switched to the low-salinity feed solution. The switching causes the change of the electrode potentials from the base potentials φ_+^H and φ_-^H to the potentials in the low salinity feed solution φ_+^L and φ_-^L, respectively. We define the potential rises $\Delta\varphi_+$ and $\Delta\varphi_-$ as the differences between the electrode potentials in the low-salinity solution and the electrode potentials in the high-salinity solution:

$$\Delta\varphi_\pm = \varphi_\pm^L - \varphi_\pm^H. \tag{1}$$

It is worth noting that the potential rise $\Delta\varphi_\pm$ depends on the concentrations of the high-salinity and low-salinity feed solutions, c_H and c_L. In Fig. 2, it can be noticed that both electrodes have a positive potential rise, i.e. $\Delta\varphi_+ > 0$ and $\Delta\varphi_- > 0$, but the electrode that has been charged at a positive potential with respect to the other has a higher potential rise, i.e. $\Delta\varphi_+ > \Delta\varphi_-$.

The cell voltage $V_{cell}(t) = \varphi_+(t) - \varphi_-(t)$ experiences a voltage rise ΔV_{cell} when the solution is changed, defined as:

$$\Delta V_{cell} = \Delta\varphi_+ - \Delta\varphi_-. \tag{2}$$

Appropriate CAPMIX electrodes require two characteristics: the ability to store charge and the existence of a cell voltage rise ΔV_{cell} upon salinity change; in turn, this feature requires that the potential rises $\Delta\varphi_+$ and $\Delta\varphi_-$ of the two electrodes are different, like in the case of the electrodes reported in Fig. 2. It is desirable that one of the electrodes has a positive potential rise and the other a negative potential rise. In the following, we will use the terms "positive-potential-rise" and "negative-potential-rise" electrodes to

refer to electrodes with positive and negative potential rise, respectively; in all the studied cases, this means that they adsorb anions and cations, respectively. The relation between the voltage rise and the salt adsorption has been recently studied [20]. It is worth noting that the notion of positive- and negative-potential-rise does not mean that the electrode is the "positive" or the "negative" electrode of a given couple, like in batteries, nor it is related to the behavior as "anode" or "cathode" in an electrochemical cell.

The energy that can be extracted per cycle is of the order of the product of the exchanged charge and the cell voltage rise ΔV_{cell}. For this reason, for CAPMIX we will select couples of electrodes with the largest difference of potential rises $\Delta\varphi_+ - \Delta\varphi_-$. This explains the importance of the concept of the potential rise for the CAPMIX technique.

3. Summary of CAPMIX experimental results

3.1. Activated carbons materials

Activated carbon is widely used in supercapacitors because of its huge surface area per gram of material, leading to high specific capacitance, and because its behavior is close to that of an ideally polarizable material.

In this section, we present experimental results obtained with four different types of activated carbon: Norit EDL Super 30, NS30 (a commercially available activated carbon) [34]; A-PC-2 (KOH activated pitch coke, KOH/coke ratio 2:1, ash free) [35]; an activated viscose rayon fabric (VRF) [36]; a steam activated polyacrilonitrile fabric (PAN) [36].

The electrodes we analyzed are 5×5 cm graphite foils, constituting the current collector, covered with a 50 μm-thick film obtained as follows. A slurry is prepared by mixing the activated carbon powder with a polymeric binder (PVDF) and the solvent (N-methyl-2-pyrrolidone). The slurry is then cast on the current collector by spraying.

The potentials of the activated carbon electrodes presented in Fig. 2 show different potential rises $\Delta\varphi_+$ and $\Delta\varphi_-$, because the EDLs on each electrode carry different types and amounts of surface charge. In fact, the potential rise strongly depends on this parameter [20]. By applying different values of the external voltage V_{ext} to the cell, it is possible to change the base potential φ^H of an electrode, i.e. its potential in the high-salinity feed solution, and thus to measure the potential rise of the electrode $\Delta\varphi$ as a function of the electrode base potential φ^H. The graph of Fig. 3 shows the relation between the potential rise $\Delta\varphi$ and the base potential φ^H for an VRF sample.

A well known problem in supercapacitors is the charge leakage: the EDLs continuously loose part of the accumulated charge, due to the recombination of the charges. This charge leakage can be expressed as a leakage current I_{leak}, provoking a loss of power of the order of $I_{leak} \bullet V_{cell}$. This leakage can lead to a reduction, or even to a complete consumption, of the extracted power.

Due to the charge leakage, the activated carbons behave as polarizable electrodes only on relatively short time scales, of the order of seconds. On longer time scales, when left in open circuit, they tend to reach a potential φ_S that is called "spontaneous potential" [22]; interestingly, they slowly come back to the same potential φ_S after charging to a different potential. This effect has been attributed to the charge leakage [22]; indeed, when the electrodes are at their spontaneous potential φ_S, the leakage vanishes. The spontaneous potential φ_S depends on the technique and the precursors used during the preparation of the material, i.e., the surface chemical properties of the electrode.

The potential rise $\Delta\varphi$ at the spontaneous potential, i.e. at $\varphi^H = \varphi_S$, is highlighted in Fig. 3. It can be noticed that a potential rise $\Delta\varphi$
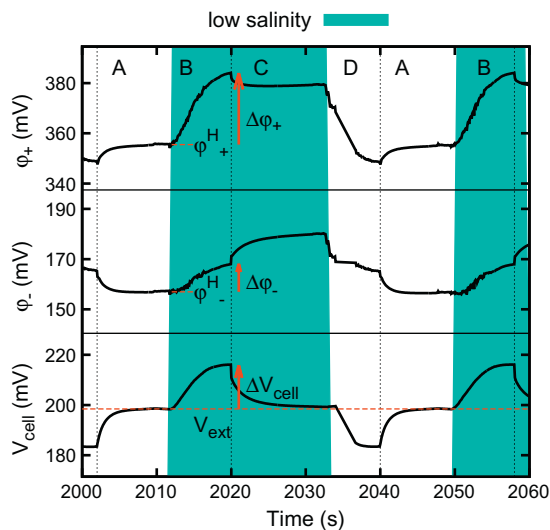
Fig. 2. Potentials $\varphi_+(t)$ and $\varphi_-(t)$ of the two electrodes as a function of time during two consecutive a CAPMIX cycles, along with the cell voltage $V_{cell}(t) = \varphi_+(t) - \varphi_-(t)$. The electrodes are identical, made of NS30 material (see Section 3.1 for the description of the materials), and are charged by means of an external power supply to V_{ext} = 200 mV.
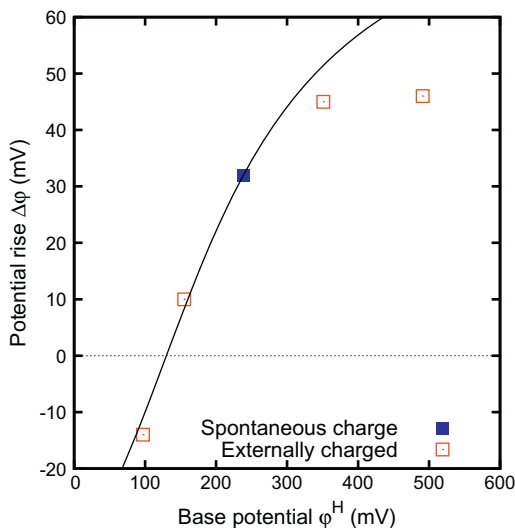
Fig. 3. Experimentally measured potential rise $\Delta\varphi$ of the VRF sample (see Section 3.1 for the description) in sodium chloride at c_H = 500 mM and c_L = 20 mM, at various base potentials φ^H. The solid line is obtained from GCS theory, Eq. (10), with C_{St} = 0.15 F/m^2 and potential of zero charge 130 mV.

is present also at the spontaneous potential, i.e. without applying any external voltage V_{ext} to the cell.

In order to obtain different potential rises from the two electrodes of a CAPMIX cell and hence a non-vanishing cell voltage rise ΔV_{cell} in a CDLE experiment, the two electrodes have to be charged at different base potentials $\varphi^H_+ \neq \varphi^H_-$, so that their potential rises become different, $\Delta\varphi_+ \neq \Delta\varphi_-$. The drawback of this approach is that the electrodes work far from their spontaneous potential φ_S, and thus they generate a charge leakage, in turn leading to a loss of power.

The precursors and the activation methods used to produce the activated carbons affect both the spontaneous potential φ_S and the potential rise $\Delta\varphi$. Some examples of the different spontaneous potentials and potential rises that can be obtained are reported in Fig. 4. It can be noticed that the various materials have different potential rises $\Delta\varphi$. It is thus possible to select suitable, different activated carbon materials spontaneously acting as positive- and
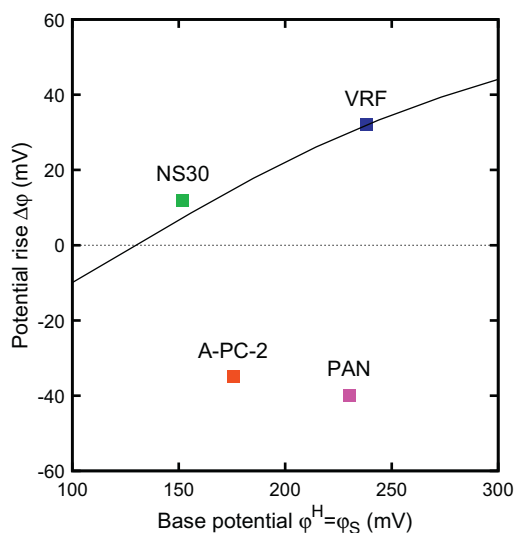
negative-potential-rise electrodes. With such electrodes, the total cell voltage rise is present, although the electrodes work close to their spontaneous potential, and their leakage is negligible. This enables a good power production [22].

A quite surprising feature that can be observed in Fig. 4 is that different materials have different potential rises, even if they are nearly at the same base potential φ^H, e.g. for NS30 and A-PC-2. This fact is confirmed by Fig. 5, showing the potentials φ_+ and φ_- of two electrodes, made of NS30 and A-PC-2 activated carbon materials. It can be clearly noticed that the potentials respond in opposite ways to the salinity changes, although the base potentials are similar.
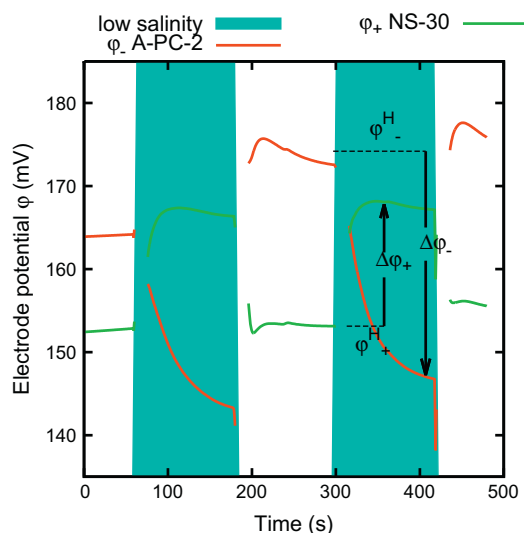
One of the fundamental properties of batteries is the cell voltage, i.e. the *difference of potentials* between the electrodes. At variance with batteries, for CAPMIX we will preferentially select couples of electrodes working nearly at the same potential (ΔV_{cell} close to 0 V), while keeping *different potential rises* $\Delta\varphi_+$ and $\Delta\varphi_-$ [22], because this leads to a technical advantage: both steps A and C are active, and the electrical circuit needed for the actual energy extraction and conversion into a continuous current does not require an "electrical flywheel" (i.e., the external power supply in the experimental setup).

For an example of this situation, see Fig. 6, showing a cycle obtained with the same materials of Fig. 5: this case shows the behavior of a cell with two different materials, having nearly the same base potential and spontaneous potential, but opposite potential rises. This behavior has been used for improving the energy extraction by means of CAPMIX technique; in the shown case, the produced power is around 50 mW/m^2.

3.2. Battery electrodes

Electrochemical batteries are the best known electrochemical charge storage devices. They can store a higher quantity of charge per unit volume, one order of magnitude more than supercapacitors, although with a lower power output, due to a higher overvoltage during the current flow [37].

A CAPMIX cell based on battery electrodes has been proposed [23]. The positive-potential-rise electrode is a gauze made of silver, and the negative-potential-rise electrode is a nanostructured $Na_{2-x}Mn_5O_{10}$ material deposited on a conductive carbon current collector. During the charge phase, silver is oxidized on the surface

Fig. 4. Graph of the potential rise $\Delta\varphi$ versus base potential φ^H, at the spontaneous potential, $\varphi^H = \varphi_S$, for various materials (see Section 3.1 for their description). The solid line is the same reported in Fig. 3.

Fig. 5. Dependence of the open-circuit potential φ_+ and φ_- of two electrodes on the salinity of the solution in which they are immersed. Results are shown for two materials (NS30 and A-PC-2, see Section 3.1 for the description). The salinities of solutions are 500 mM and 20 mM of NaCl. The produced power is 50 mW/m^2.
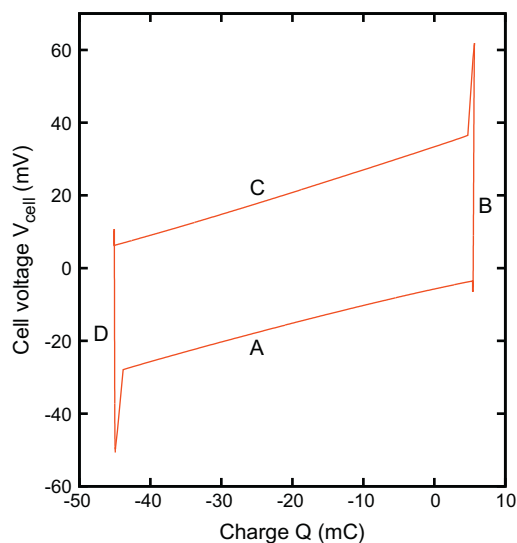
Fig. 6. Voltage *versus* charge graph for the CAPMIX cycle performed with NS30 and A-PC-2 materials, the same couple of Fig. 5. The charging and discharging phases are performed by connecting the electrodes through a load, 10 Ω in the high-salinity solution (c_H = 500 mM of NaCl) and 40 Ω in the low-salinity solution (c_L = 20 mM of NaCl). No external power supply is needed, V_{ext} = 0 V.

Fig. 7. Behavior of three kinds of battery electrodes, used in a CAPMIX cycle, in the potential rise *versus* base potential [23] graph. The concentrations of the solutions are c_H = 600 mM and c_L = 25 mM. The solid lines are the obtained by Eq. (18), a consequence of Nernst equation.

of the gauze, and the Cl⁻ ions are stored in the form of insoluble AgCl. The half-reaction is thus:

$$Ag + Cl^- \rightarrow AgCl + e^-. \tag{3}$$

On the $Na_{2-x}Mn_5O_{10}$ electrode, Na^+ ions are reduced and get intercalated inside the crystalline structure:

$$5MnO_2 + 2Na^+ + 2e \rightarrow Na_2Mn_5O_{10}. \tag{4}$$
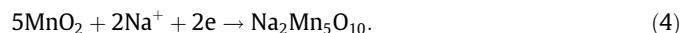
The potential of the two electrodes depends on the activity of the ions that participate in the redox reactions, i.e. Cl⁻ and Na⁺ in this case. When the concentration of the ions is increased from c_L = 25 mM to c_H = 600 mM, the potential of the $Na_{2-x}Mn_5O_{10}$ electrode increases by around 65 mV, and the potential of the silver electrode decreases by around 50 mV. The behavior of the electrodes in the potential rise *versus* base potential graph is shown in Fig. 7. The overall voltage of the cell composed by the silver and $Na_{2-x}Mn_5O_{10}$ electrodes increases by around ΔV_{cell}=115 mV. Such a cell has been applied in a CAPMIX-like cycle; in the first experiments, a power of the order of 200 mW per square meter of electrode has been obtained [23].
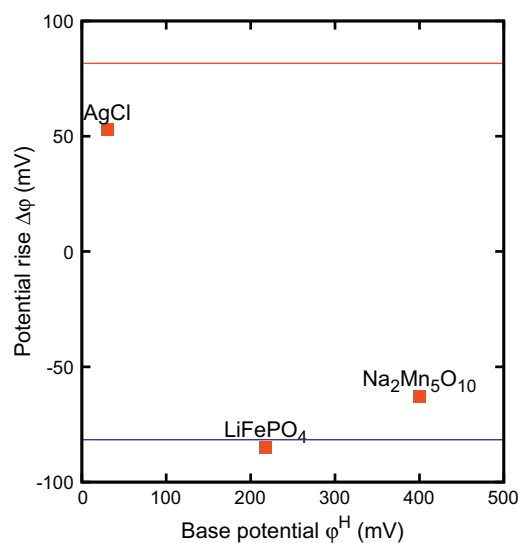
The same concept can be applied to other materials used for batteries, profiting on the wide knowledge on this topic. For example, an intercalating material developed for lithium batteries is LiFePO₄. This material has been successfully used in a CAPMIX-like cycle with a solution of LiCl [23]; results for this material are also reported in Fig. 7. A concentrated solution of this salt has a quite high boiling point elevation, and thus it can be usefully applied in conjunction with the closed cycles for thermoelectrical energy conversion, e.g. for solar applications.

For CAPMIX applications, the main of the pros of battery electrodes is the long self-discharge time, which avoids the negative effects of the current leakage. The lower power output is among the cons.

4. Models

4.1. Ideally polarizable electrodes

Activated carbon materials can be modeled as polarizable electrodes, at least on the time scales of the seconds. The material is modeled as a locally flat conductor, with a surface charge σ^0, dipped into a solution containing ions. We assume that the surface charge σ^0 can be changed by connecting the conductor to a power supply; moreover, we assume that σ^0 does not change when the conductor is isolated, i.e. we assume that the material can be treated as "polarizable".

Various charged layers can be identified in the solution close to the electrode surface. Following Ref. [38], we assume that, at a distance β from the conductor surface, there is a flat charge distribution σ^i, which will be better specified below. Still further from the surface, at a distance $\beta + \gamma$ and beyond, ions undergoing only electrostatic interactions with the surface are located; they are also subjected to collisions with solvent molecules, so that they are in fact distributed over a certain distance to the solid. Such charges represent the so-called "diffuse layer", with a total charge σ^d [39]. The structure of the layers is shown in Fig. 8. This scheme can be used for describing various models present in literature [40–43]. In particular, the condition $\sigma^i = 0$ and $\beta = \gamma = 0$ represents the absence of a Stern layer, and $\beta = 0$ represents molecules adsorbed at the same plane of σ_0.

Since the whole system is electrically neutral, the following equation holds:

$$\sigma^0 + \sigma^i + \sigma^d = 0. \tag{5}$$

The potential φ is φ^0 inside the conductor, and we assume that, at infinity, the potential vanishes. From $x = 0$ to $x = \beta$, the potential φ decreases linearly down to φ^i:

$$\varphi^i = \varphi^0 - \sigma^0 \frac{\beta}{\beta + \gamma} \frac{1}{C_{St}}, \tag{6}$$

where $C_{St} = \epsilon_0 \epsilon_r/(\beta + \gamma)$ is the Stern layer specific capacitance, ϵ^0 is the dielectric constant and ϵ_r is the relative dielectric constant of the solvent. Then, from $x = \beta$ to $x = \beta + \gamma$, the potential φ decreases linearly down to φ^d:

$$\varphi^d = \varphi^i - (\sigma^0 + \sigma^i) \frac{\gamma}{\beta + \gamma} \frac{1}{C_{St}}. \tag{7}$$

The following sections will discuss various physical origins of the charged layer and its effect on the CDLE phenomenon.
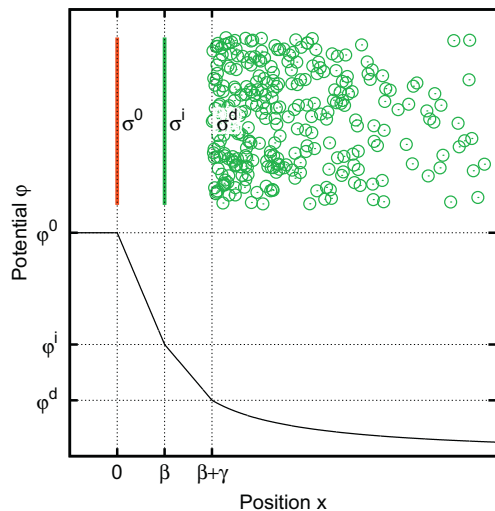
Fig. 8. Potential distribution in the different parts of the EDL. The surface charge σ^0 is at position 0. The adsorbed charge σ^i is at position β. The diffuse charge σ^d is distribute at positions $x > \beta + \gamma$.

The goal is to calculate the function $\varphi^0(\sigma^0, c)$, depending on the stored charge σ^0 and the salinity c. In turn, this function will be used to calculate the potential rise $\Delta\varphi$ between the salinities c_H and c_L:

$$\Delta\varphi = \varphi^0(\sigma^0, c_L) - \varphi(\sigma^0, c_H), \tag{8}$$

and the base potential φ^H:

$$\varphi^H = \varphi^0(\sigma^0, c_H). \tag{9}$$

The two equations represent the dependence of $\Delta\varphi$ on φ^H, given in a parametric form, where σ^0 is the parameter.

It is worth noting that, in this case, it is not possible to define a "spontaneous potential". Instead, the potential rise will depend on the charge status of the electrode, i.e. on σ^0. For each electrode in a given solution, there will be a line on the potential rise *versus* base potential graph.

4.2. Gouy–Chapman–Stern model

In the simplest case, we can assume $\sigma^i = 0$. The layer with thickness $\beta + \gamma$ is simply a charge-free layer [38], i.e. a layer in which the ions cannot enter due to their steric hindrance.

As a further approximation, we assume that the electrodes are flat, i.e. we neglect the presence of pores. As we will see, this extremely simplified model qualitatively explains some of the observed phenomena. Under these assumptions, Gouy–Chapman–Stern (CGS) theory gives a relation between σ^d and φ^d:

$$\sigma^d = -\sqrt{8\epsilon_0 \epsilon_r cRT} \sinh\left(\frac{zF\varphi^d}{2RT}\right), \tag{10}$$

where R is the gas constant, T is the temperature, F is the Faraday constant, and c is the salinity expressed in moles per unit of volume. Eq. (10) has been written with the further simplification that the salts dissociate into two ions, with the same absolute value of charge z (symmetrical electrolytes): this is valid for the case of solutions of NaCl, one of the main solutes of the sea water. However, the presence of multi-valent ions, also present in the sea water, can be easily handled by the GCS model, see for example Ref. [44].

From the electro-neutrality Eq. (5) and the condition $\sigma^i = 0$, we obtain $\sigma^d = -\sigma^0$. In turn, from σ^d we calculate φ^d by means of Eq. (10). Finally, by using the Eqs. (6) and (7), with $\sigma^i = 0$, we obtain φ^0:

$$\varphi^0 = \varphi^d + \frac{\sigma^0}{C_{St}}. \tag{11}$$

The relation between φ^0 and σ^0 is shown in Fig. 9a. Panel b shows the potential rise $\Delta\varphi$ *versus* base potential φ^H plotted parametrically with the same equations. The GCS theory describes the CDLE phenomenon, i.e. the dynamics of the EDL during the changes of concentration: a positively charged EDL experiences a positive potential rise and *vice versa* [14].

It is worth noting that, under the present approximation, the potential of zero charge, i.e. the value of φ^0 at which $\sigma^0 = 0$, corresponds to the vanishing of the potential rise, i.e. $\Delta\varphi = 0$.

Some predictions of the GCS model are compared to experimental results in Fig. 3, where qualitative agreement is obtained. The voltage rise observed in experiments is lower than the predicted by GCS model due to the finite ion size of ions, that prevents the high concentrations in the diffuse part of the EDL predicted by the GCS model [33,45,21], thus limiting the maximum voltage rise.
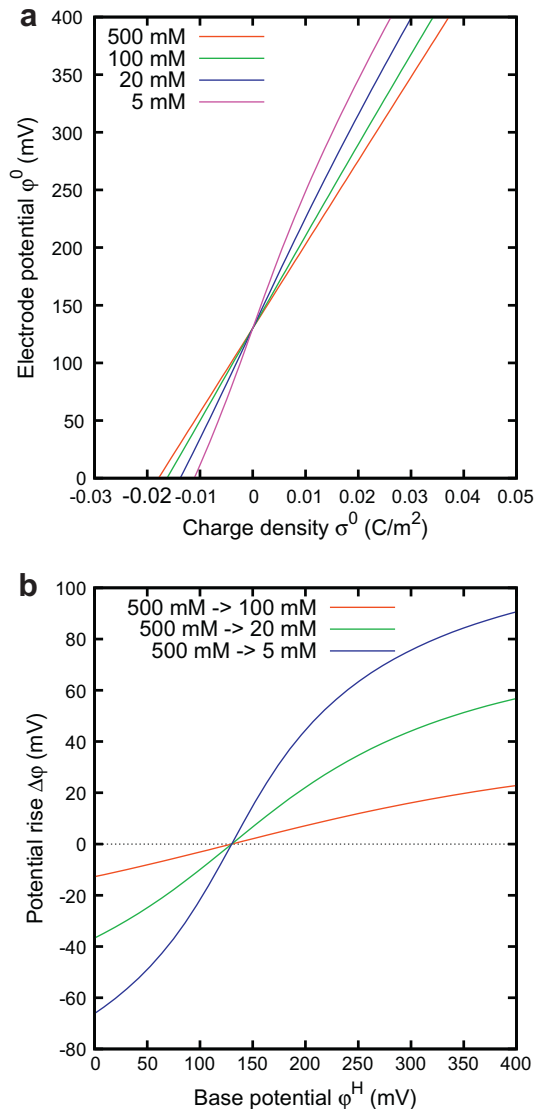
Fig. 9. Calculated results of GCS model. Panel a: potential φ^0 *versus* surface charge σ^0. Panel b: potential rise $\Delta\varphi$ *versus* base potential φ^H. Specific Stern layer capacitance: $C_{St} = 0.15$ F/m²; potential of zero charge: 130 mV.

4.3. Permanently adsorbed charged molecules and solvent polarization

Fig. 10a is a sketch showing the presence of a charged Stern layer, that physically correspond to a layer of permanently adsorbed charged molecules.

This case is modeled by considering σ^i as a non-vanishing constant. In order to calculate the dependence of φ^0 on σ^0, we first evaluate σ^d by means of the electro-neutrality Eq. (5):

$$\sigma^d = -\sigma^0 - \sigma^i. \tag{12}$$

Then, by means of Gouy–Chapman formula Eq. (10), we calculate φ^d. Finally, φ^0 is obtained from the combination of the Eqs. (6) and (7).

The effect of the presence of a charged layer on the potential versus charge graph is shown in Fig. 11a. It can be clearly seen that the effect is a translation on both charge and potential axes. In the potential rise versus base potential graph, reported in panel b, the effect of the charged layer is a translation along the base potential axis.

Considering two materials, prepared with different adsorbed charged molecules, as in Fig. 11b, it is possible to charge them at the same base potential, e.g. the value indicated by the vertical

dashed line, while keeping different potential rises. In this case, the two materials present different potential rises, one positive and one negative, although they have the same base potential. This model qualitatively explains one of the phenomena shown in Figs. 4 and 5, i.e. the presence of materials with different sign of the potential rise, at the same base potential.

In the present situation, the vanishing of the potential rise, i.e. $\Delta\varphi = 0$, corresponds to the condition $\sigma^0 + \sigma^i = 0$, i.e. to the situation at which the sum of the surface charge and the charge of the adsorbed molecules vanishes. This also corresponds to the condition that $\sigma^d = 0$, representing the absence of a diffuse EDL: indeed, the potential rise is a consequence of the expansion of the diffuse EDL (CDLE phenomenon).

Another effect that is considered in the discussion of EDLs is the polarization of the solvent [38], that is sketched in Fig. 10b. The polar molecules of the solvent (e.g. water) that are close to the surface of the conductor acquire a preferential orientation. Assuming that the polar molecules are preferentially oriented so that their positive side is towards the conductor, the positive sides of the polar molecules form a positively charged layer close to the conductor. Also this layer can be roughly modeled as a surface charge σ^i. The effect of the solvent polarization is thus similar to the presence
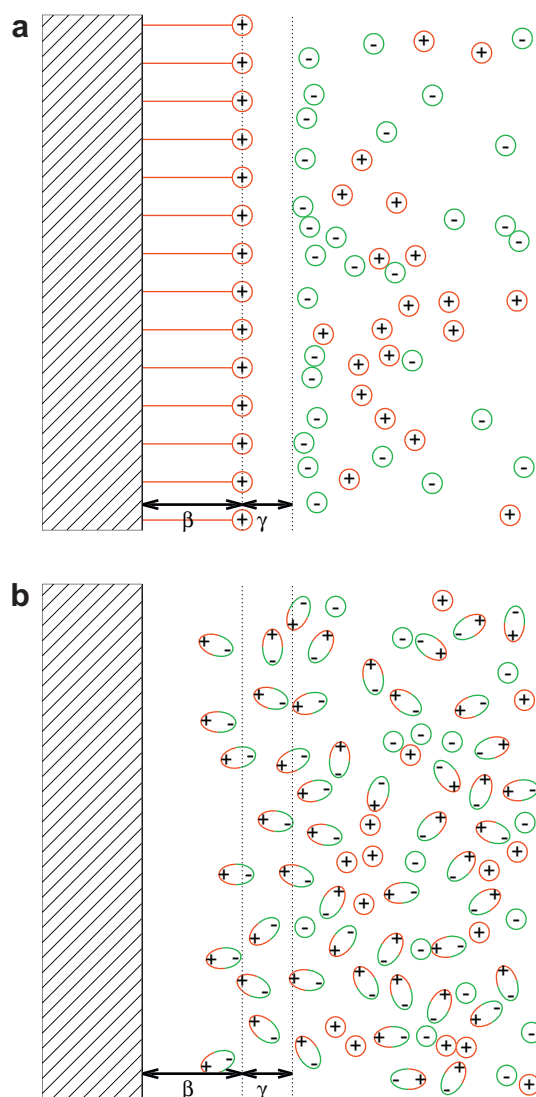

Fig. 10. Sketch of the double layer. Panel a: charged molecules permanently adsorbed on the surface. Panel b: solvent polarization.
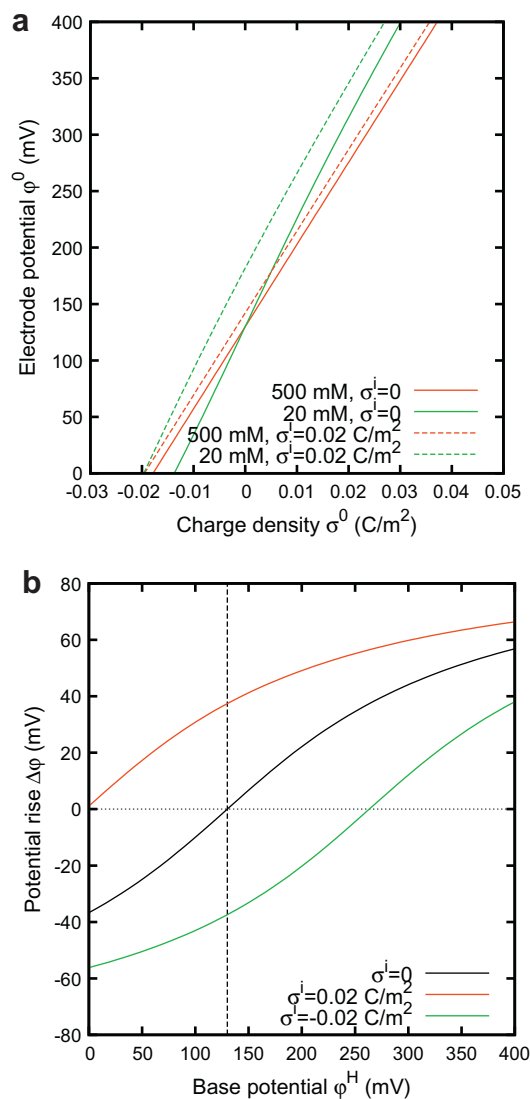

Fig. 11. Calculation of the effect of a charged layer, with a fixed surface charge σ^i. Specific Stern layer capacitance: $C_{St} = 0.15$ F/m^2; $\gamma = 0$. When $\sigma^i = 0$ the potential of zero charge is 130 mV.

of permanently adsorbed charged molecules, that manifests as a translation along the base potential axis in the potential rise *versus* base potential graph.

4.4. Specific adsorption

This case refers to the situation in which one of the ions in solution binds reversibly to the surface of the conductor, with a given reaction constant. The relation between σ^i and φ^i is given by [38]:

$$\sigma^i = \frac{z_i e N_s K_i e^{-\frac{z_i F \varphi^i}{RT}} c}{1 + K_i e^{-\frac{z_i F \varphi^i}{RT}} c}, \tag{13}$$

where N_s is the surface density of binding sites, K_i is the binding constant and z_i is the charge of the adsorbed ions.

Fig. 12a shows the resulting potential *versus* charge graph. In order to better appreciate the shapes of the curves, the quantity σ/C_{St} has been subtracted from the potentials. It can be noticed that the curves no more meet in a single point, as in the previous cases.
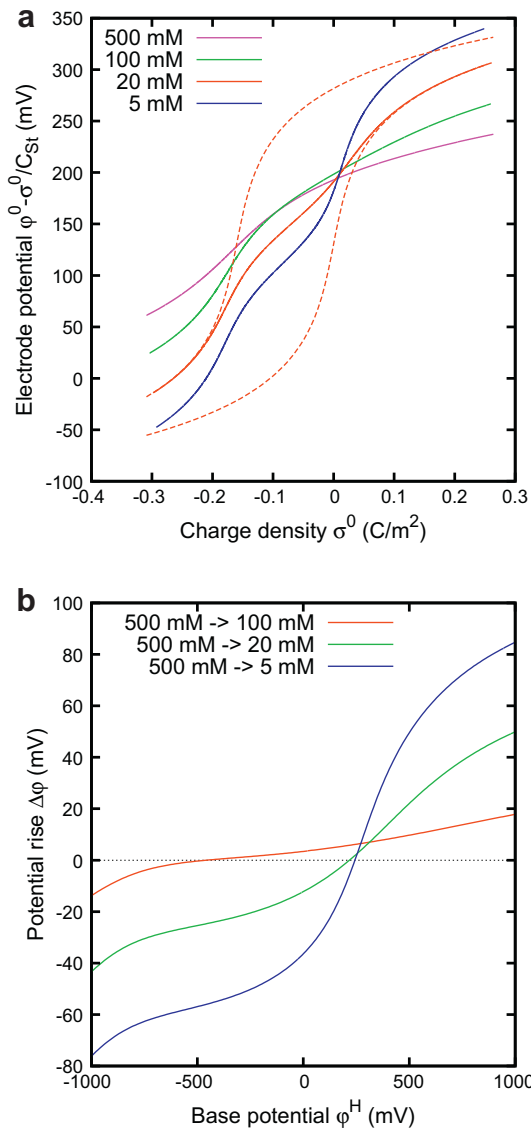
Fig. 12. Calculation of the effect of a charged layer due to reversibly adsorbed molecules. In order to improve the representation of the potential in panel a, the quantity σ/C_{St} has been subtracted. The dotted lines represent the limiting values for $\varphi^i \to \pm\infty$ expressed in Eq. (14). Specific Stern layer capacitance: $C_{St} = 0.15$ F/m²; potential of zero charge for $\sigma^i = 0$: 130 mV; $\gamma = 0$.

In order to qualitatively explain this behavior, we consider two limiting cases. In the following calculation, we assume $z_i > 0$, without loosing generality.

In the limit $\varphi^i \to +\infty$, σ^i vanishes. This corresponds to the absence of the charged layer: the electric field repels the ion so strongly, that it cannot bind to the surface, even if the binding could be chemically favored.

In the limit $\varphi^i \to -\infty$:

$$\sigma^i \to z_i e N_s. \tag{14}$$

This limit corresponds to a charged layer of permanently adsorbed molecules: the chemical binding helps the formation of a nearly permanent charged layer.

Both limits can be calculated as described in the previous sections. The corresponding limiting curves are plotted in Fig. 12a as dotted lines, for the concentration 20 mM. It can be noticed that the solid curve, i.e. the curve obtained with the complete theory, asymptotically approaches one of the limiting curves for each side, and moves from one to the other in between.

Fig. 12b presents the potential rise *versus* base potential graph. It can be noticed that the vanishing of the potential rise, i.e. $\Delta\varphi = 0$, takes place at different base potentials for different salinities. This means that the vanishing of the potential rise does not take place at the base potential corresponding to the potential of zero charge; indeed, in the present case, the potential of zero charge actually depends on the concentration of the ions that reversibly become adsorbed.

4.5. Non-polarizable electrodes

The battery electrodes are modeled as ideally polarizable electrodes, on which a single redox reaction takes place. This is often the case, from a practical point of view, because a single redox reaction has an exchange current that is much higher than other possible reactions. When used in a CAPMIX cell, the dependence of the electrode potential on the ion activity basically corresponds to the half-cell potential used in electrochemistry, which is expressed by the Nernst equation:

$$\varphi = \varphi_0 - \frac{RT}{zF} \ln\left(\frac{a_{ox}}{a_{red}}\right), \tag{15}$$

where φ_0 is the standard half-cell reduction potential, z is the number of electrons transferred in the reaction, and a_{ox} and a_{red} are the activities of respectively the oxidized and reduced species.

Approximating the activity with the concentration is often a good approximation, and gives qualitatively valid results for the solutions used in Section 3:

$$\varphi = \varphi_0 - \frac{RT}{zF} \ln\left(\frac{c_{ox}}{c_{red}}\right). \tag{16}$$

In the case of battery electrodes, there is a single, well defined value of the base potential, as in Fig. 7, that cannot be changed even by adding a charge to the electrode. This potential is given by:

$$\varphi^H = \varphi_0 - \frac{RT}{zF} \ln\left(\frac{c_H}{c_{reference}}\right), \tag{17}$$

where $c_{reference}$ is 1 M.

In order to calculate the potential rise, we assume that the ion species which is accumulated in the electrode does not change its concentration during the solution change. The result is thus:

$$\Delta\varphi = s \frac{RT}{zF} \ln\left(\frac{c_H}{c_L}\right). \tag{18}$$

where $s = 1$ for the electrode interacting with anions, and $s = -1$ for the electrode interacting with the cations.

Fig. 13 shows the position in the potential rise *versus* base potential graph of various redox reactions, calculated from the Nernst equation and the table of reduction potentials.

It can be noticed that, once the solute and the concentrations c_H and c_L are defined, the potential rise should not depend on the electrode material and the redox reaction taking place. The predictions from Nernst equation are reported in Fig. 7. The measured values are slightly closer to 0 V, leading to an electrochemical efficiency of the energy extraction cycle less than 1. However, it is worth noting that, in the case of the battery electrode materials that work by intercalating the sodium ions, the potential depends also on the charging status, i.e. on the concentration of the sodium ions inside the material.

4.6. Parasitic redox reactions

A usual finding concerning supercapacitors is the presence of a charge leakage, consisting in a slow discharge of a supercapacitor when it first charged and then it is left in open circuit. Indeed, this effect can be seen also in experiments with any couple of activated carbon electrodes in a salt solution. For example, in Fig. 3, the two electrodes are initially at the same potential. We call this initial potential "spontaneous potential", φ^S, and, for this case, it is around 238 mV. When the cell is then charged, the potentials of the two electrodes become different. If the cell is left in open circuit, the cell voltage comes back to 0 V, and the potentials of the two electrodes tend to come back to φ^S.

The leakage actually consists in a current which flows through the EDL, thus discharging it. The leakage is mainly due to redox reactions taking place on the surface of an electrode, which thus becomes non-ideally polarizable. It is not necessary that the redox reaction involve the ions of the dissolved salt; on the contrary, it can involve an unwanted chemical species. For example, in the case of activated carbon electrodes in water solutions, it has been proposed [24] that one of the redox reactions taking place on the surface of the carbon involves quinone groups: in this case, only the H^+ ions are involved in the reaction. Other redox reactions that have been proposed are the carbon oxidations and reactions involving the water molecules [24]. Some of them require molecular oxygen in solution; indeed, we experimentally observed that
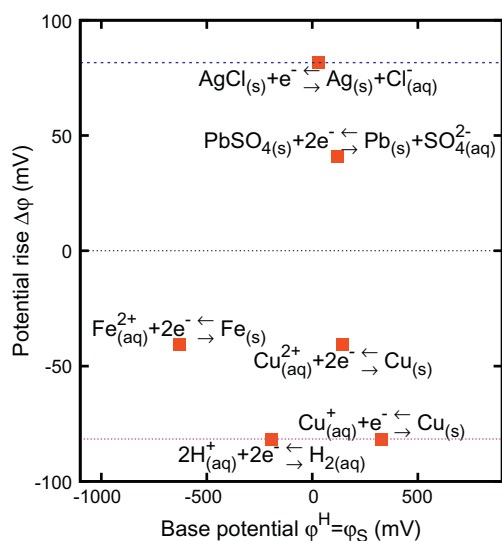
removing oxygen by bubbling nitrogen partially reduces the leakage. Moreover, we noticed that another effect of bubbling nitrogen is that φ^S becomes lower when the solution is de-oxygenized by bubbling nitrogen, and it becomes even lower when sodium meta-bisulfite 0.25 mM is added to the solution. This suggests that some of the redox reactions involve surface groups that are formed by reactions involving oxygen.

The simultaneous presence of a nearly polarizable electrode, with parasitic redox reactions, is described by the electrical circuit shown in Fig. 14. The potential of the battery equals φ^S. The leakage takes place through the resistor R_{leak}. The capacitance of the polarizable electrode is C. The equation governing the capacitor voltage φ_C is:

$$\frac{d\varphi_C}{dt} = \frac{1}{C}\left[I + \frac{\varphi^S - \varphi_C}{R_{leak}}\right]. \tag{19}$$

The solution of this equation is a decreasing exponential, approaching φ^S. Experimentally, it can be noticed that the characteristic time is of the order of 10^4 s. Since it is equal to $C \bullet R_{leak}$, the characteristic time defines the leakage resistance. This view is extremely simplified, since it neglects the strong non-linearity of the leakage, but it is enough for describing the behavior around the spontaneous potential. Basically, the electrode is immersed in the concentrated solution, and reaches the spontaneous potential φ^S with a characteristic time $C \bullet R_{leak}$. When the solution is changed, the potential rise takes place in a much shorter time, of the order of the seconds; on this time scale, the electrode behaves as polarizable, and the potential rise is simply the potential rise of a polarizable electrode with a base potential $\varphi_0 = \varphi^S$.

The potential φ^S depends on the activity of the molecules involved in the redox reaction. We consider, for example, the following reaction:

$$Q + 2H^+ + 2e^- \rightarrow QH_2, \tag{20}$$

where Q is a quinone group and QH_2 is the corresponding hydroquinone. The potential φ^S is thus given by the Nernst equation, and depends only on the activity of the H^+ ion. Since the pH of the solution is independent on the concentration of NaCl, also φ^S does not depend on the salinity.

The model presented in this section can explain one of the features that can be observed in Fig. 4, where various materials are reported in the potential rise $\Delta\varphi$ *versus* base potential φ^H graph. Two of them (NS30 and VRF) fall nearly on the same GCS theoretical line (solid line): it is thus apparent that they have similar properties, but different spontaneous potentials φ^S, that, in the present section, is identified with the potential shown in Fig. 14. The other two materials fall on totally different GCS theoretical lines; in that
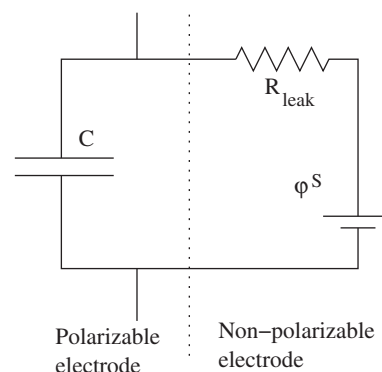
Fig. 13. Base potentials and potential rises of various redox reactions, calculated from the table of the reduction potentials and Nernst equation. The potentials are measured with respect to the 3 M Ag/AgCl reference electrode. The concentrations are $c_H = 600$ mM and $c_L = 25$ mM, and refer to the ion present in the reaction equation.

Fig. 14. Electrical circuit describing the polarizable electrode with parasitic redox reactions leading to leakage.

case, the difference is ascribed to the presence of a layer of charged adsorbed molecules.

5. Conclusions

In this paper, we have analyzed a wide set of experimental results focusing on the parameters that determine the performance of a CAPMIX cell, namely, the voltage rise upon salinity change and the base potential. These two parameters can vary over a wide set of values and combinations, and hence several theoretical environments had to be considered in order to obtain a fair understanding of all the possibilities.

When polarizable electrodes are considered, like in the case of activated carbon electrodes, the consideration of redox reactions serve us to model the charge leakage and justify the spontaneous potentials of the activated carbon electrodes. The potential rise of the activated carbon electrodes is explained by Gouy–Chapman–Stern theory, although some refinements are needed in order to achieve a total description. In particular, the presence of different activated carbon electrodes with different potential rises at nearly the same base potential has been described in terms of permanent or reversible adsorption of charged molecules. Moreover, we have shown that the presence of redox reactions, modeled with Nernst equations, is enough to give a qualitative explanation of the observed base potentials and the potential rises of battery electrodes.

Acknowledgments

References

[1] R.E. Pattle, Nature 174 (1954) 660.
[2] R.W. Norman, Science 186 (1974) 350–353.
[3] B.E. Logan, M. Elimelech, Nature 488 (2012) 313–319.
[4] J. Kuleszo, C. Kroeze, J. Post, B.M. Fekete, J. Integr. Environ. Sci. 7 (2010) 89–96.
[5] S. Loeb, Desalination 120 (1998) 247–262.
[6] M. Turek, B. Bandura, P. Dydo, Desalination 221 (2008) 462–466.
[7] A. Cipollina, A. Misseri, G. D'Alí Staiti, A. Galia, G. Micale, O. Scialdone, Desalination Water Treat. 49 (2012) 390–403.
[8] R.L. McGinnis, J.R. McCutcheon, M. Elimelech, J. Membr. Sci. 305 (2007) 13–19.
[9] O. Levenspiel, N. de Vevers, Science 183 (1974) 157–160.
[10] S. Loeb, Science 189 (1975) 654–655.
[11] T.S. Chung, X. Li, R.C. Ong, Q.G.H. Wang, G. Han, Curr. Opin. Chem. Eng. 1 (2012) 246–257.
[12] J.N. Weinstein, F.B. Leitz, Science 191 (1976) 557–559.
[13] J.W. Post, H.V.M. Hamelers, C.J.N. Buisman, Environ. Sci. Technol. 42 (2008) 5785–5790.
[14] D. Brogioli, Phys. Rev. Lett. 103 (2009) 058501.
[15] B.B. Sales, M. Saakes, J. Post, C.J.N. Buisman, P.M. Biesheuvel, H.V.M. Hamelers, Environ. Sci. Technol. 44 (2010) 5661.
[16] D. Brogioli, R. Zhao, P.M. Biesheuvel, Energy Environ. Sci. 4 (2011) 772–777.
[17] O. Burheim, B. Sales, O. Schaetzle, F. Liu, H.V.M. Hamelers, Auto generative capacitive mixing of sea and river water by the use of membranes, in: ASME 2011 International Mechanical Engineering Congress and Exposition (IMECE2011) (Denver, Colorado, USA), 2011, pp. 483–492, doi: 10. 1115/IMECE2011-63459, (paper no. IMECE2011-63459).
[18] M.F.M. Bijmans, O.S. Burheim, M. Bryjak, A. Delgado, P. Hack, F. Mantegazza, S. Tennisson, H.V.M. Hamelers, Energy Procedia 20 (2012) 108–115.
[19] R.A. Rica, R. Ziano, D. Salerno, F. Mantegazza, R. van Roij, D. Brogioli, Entropy 15 (2013) 1388–1407.
[20] R.A. Rica, R. Ziano, D. Salerno, F. Mantegazza, D. Brogioli, Phys. Rev. Lett. 109 (2012) 156103.
[21] N. Boon, R. van Roij, Mol. Phys. 109 (2011) 1229–1241.
[22] D. Brogioli, R. Ziano, R.A. Rica, D. Salerno, O. Kozynchenko, H.V.M. Hamelers, F. Mantegazza, Energy Environ. Sci. 5 (2012) 9870–9880.
[23] F. La Mantia, M. Pasta, H.D. Deshazer, B.E. Logan, Y. Cui, Nano Lett. 11 (2011) 1810–1813.
[24] S. Porada, R. Zhao, A. van der Wal, V. Presser, P.M. Biesheuvel, Prog. Mater. Sci., 2013, (in press), http://dx.doi.org/10.1016/j.pmatsci.2013.03.005.
[25] P.M. Biesheuvel, A. van der Wal, J. Membr. Sci. 346 (2010) 256–262.
[26] M. Pasta, C.D. Wessells, Y. Cui, La Mantia, Nano Lett. 12 (2012) 839–843.
[27] F. Liu, O. Schaetzle, B.B. Sales, M. Saakes, C.J.N. Buisman, H.V.M. Hamelers, Energy Environ. Sci. 5 (2012) 8642–8650.
[28] O.S. Burheim, F. Liu, B.B. Sales, O. Schaetzle, C.J.N. Buisman, H.M. Hamelers, J. Phys. Chem. C 116 (2012) 19203–19210.
[29] B.B. Sales, O.S. Burheim, F. Liu, O. Schaetzle, C.J.N. Buisman, H.V.M. Hamelers, Environ. Sci. Technol. 46 (2012) 12203–12208. doi: 10.1021/es302169c.
[30] R.A. Rica, D. Brogioli, R. Ziano, D. Salerno, F. Mantegazza, J. Phys. Chem. C 116 (2012) 16934–16938.
[31] R.A. Rica, R. Ziano, D. Salerno, F. Mantegazza, M.Z. Bazant, D. Brogioli, Electrochimica Acta 92 (2013) 304–314.
[32] B.B. Sales, F. Liu, O. Schaetzle, C.J.N. Buisman, H.V.M. Hamelers, Electrochimica Acta 86 (2012) 298–304. doi: 10. 1016/j.electacta.2012.05.069..
[33] M.L. Jiménez, M. M. Fernández, S. Ahualli, G. Iglesias, A.V. Delgado, J. Colloid Interface Sci. 402 (2013) 340–349.
[34] Produced by Norit Activated Carbon, CABOT Inc., http://www.norit.com/.
[35] Kindly provided by M. Bryjak, Wrocław University of Technology, Department of Polymer and Carbon Materials, Poland; http://www.portal.pwr.wroc.pl.
[36] Kindly provided by O. Kozynchenko, MAST Carbon International Limited; www.mastcarbon.co.uk.
[37] P.F. Ribeiro, B.K. Johnson, M.L.C. et al., Proceedings of the IEEE vol. 89, 2001, pp. 1744–1756.
[38] J. Lyklema, Fundamentals of Interface and Colloid Science, vol. 2, Academic press, New York, 1995.
[39] A.V. Delgado (Ed.), Interfacial Electrokinetics and Electrophoresis, Marcel Dekker, New York, 2002.
[40] P.M. Biesheuvel, J. Phys.: Condens. Matter 16 (2004) L499–504.
[41] P. Biesheuvel, J. Colloid Interface Sci. 275 (2004) 514–522.
[42] K. Köhler, P.M. Biesheuvel, R. Weinkamer, H. Möhwald, G.B. Sukhorukov, Phys. Rev. Lett. 97 (2006) 18830.
[43] P. Biesheuvel, T. Mauser, G. Sukhorukov, H. Möhwald, Macromolecules 39 (2006) 8480–8486.
[44] R. Zhao, M. van Soestbergen, H.H.M. Rijnaarts, A. van der Wal, M.Z. Bazant, P.M. Biesheuvel, J. Colloid Interface Sci. 384 (2012) 38–44.
[45] M.Z. Bazant, M.S. Kilic, B.D. Storey, A. Ajdari, Adv. Colloid Interface Sci. 152 (2009) 48–88.